NKFIH FK project no. 128741

Final report

Principal investigator: Attila Virág

Co-investigators: Viktor Karádi, Piroska Pazonyi, Bence Szabó

The fossil members of the genus *Spermophilus* (Rodentia: Sciuridae: Xerinae) first appeared during the late Pliocene (2.6 Ma) and reached a peak of abundance in the Late Pleistocene and Holocene, revealing a group nearly as diverse as found today. The westernmost occurrence of the genus is restricted to Central Europe, where it is represented by European ground squirrel, *S. citellus*. During the Middle Pleistocene – early Holocene, these areas were inhabited by the morphologically similar but presently extinct *S. citelloides*. This species was first described more than a century ago by Tivadar Kormos from the classical Hungarian Late Pleistocene fossil locality, Pilisszántó Rock Shelter (Kormos 1915).

Prior to our study, *S. citelloides* was considered amongst the least known ground squirrel species that still required reassessment in a modern phylogenetic and taxonomic framework. Therefore, a detailed description of the cranial and dental morphology was made for the species by Maxim Sinitsa (see Sinitsa et al. 2021). Its phylogenetic relationships were assessed by a cladistic analysis based on a standard cranial character matrix (that of Sinitsa et al. 2019). The analysis was run in *TNT v.1.1*. The tree turned out to be fairly congruent with molecular-based phylogenies of the genus and related marmotine taxa (e.g. Harrison et al. 2003, Herron et al. 2004, Ermakov et al. 2015). Only one derived character (namely the strong posterior convergence of the upper tooth rows; character 27, state 2) separates *S. citelloides* from *S. suslicus*, which indicates a relatively short morphological distance between these species. Together, they form a clade that is weakly supported by a reversal (i.e. rather than being close to the ventral edge, the mental foramen is located roughly at the middepth of the diastemal portion of the mandible; character 51, state 1).

As a part of the NKFIH FK128741 project, we performed a geometric morphometric (GM) analysis on the occlusal outline of the teeth belonging to the taxa, which proved to be closely related to *S. citelloides* during the cladistic analysis. For this aim, a total of 2013 teeth from 500 individuals belonging to six different species were photographed in occlusal view (Tab. 1).

Table 1. *Specimens involved in the geometric morphometric analysis of ground squirrels.*

-	specimens	teeth	p4	m1	m2	m3	P3	P4	M1	M2	M3
S. alashanicus	7	63	7	7	7	7	7	7	7	7	7
S. citelloides	349	995	210	251	157	157	7	23	39	37	20
S. citellus	55	245	5	55	5	5	5	5	55	55	5
S. dauricus	17	154	17	17	16	16	17	18	18	18	17
S. suslicus	59	451	38	69	38	38	37	36	64	65	37
S. xanthoprymnus	13	105	11	11	9	9	12	13	13	13	12
TOTAL	500	2013	288	410	232	232	85	102	196	195	98

The initial digitisation of the outlines was done manually by placing a succession of approximately 50-90 shape descriptors along the contour of each tooth using the multi-point tool of *ImageJ v1.52a* (Fig. 1A). A consistent, easily recognisable starting place (e.g. the deepest point in an anatomically meaningful indentation) was defined for each tooth position and the subsequent points were put up in a clockwise manner in the case of left and in an anticlockwise manner in the case of right teeth. To avoid bias induced by bilaterality, the point configurations acquired from left teeth were mirrored into their right counterparts. To achieve uniform point allocation, the manually placed shape descriptors were rarefied to 40 points on each outline using the *equidistantCurve()* function of the *Morpho* package (Schlager 2017) within the *R v.3.5.2.* programming environment (R Core Team 2013; Fig 1B). During the next step, a custom automated algorithm identified indentations and protrusions of the outlines, utilising the fact that if a roughly circular shape is expressed as a function of the distances of its points from the shape centroid, changes in the sign of its first order derivative correspond to the inflections in the original contour. From these, only points, which were consistently traceable on all studied teeth of the same type were retained as landmarks (LMs). The finer details of the intermediate contour segments were recorded by 1-10 equidistant semilandmarks (SLMs; Fig. 1C). Their exact number was defined based on the average length of a given section. The precise configuration is depicted on Fig. 2 for each tooth position.

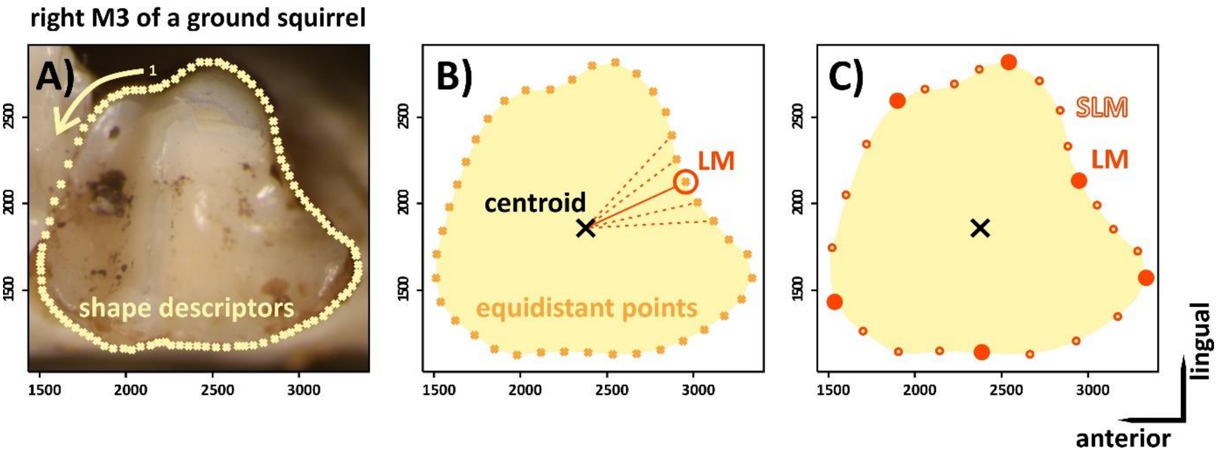

Figure 1. *Initial shape descriptors (**A**), resampled equidistant points (**B**) and the final landmark (LM) and semilandmark (SLM) configuration (**C**) shown in the case of a right M3 of a ground squirrel.*

Variation due to the size and orientation of the teeth and their location on the image were eliminated using a generalised Procrustes superimposition, during which the landmark configurations were translated to a common origin, scaled to unit centroid size, and iteratively rotated until the sum of squared Euclidean distances among the homologous points became minimal. The resulting Procrustes shape coordinates formed the basis of a canonical variate analysis (CVA) for each tooth position (Fig. 3) implemented by the *CVA()* function of the *Morpho* package of *R*. Centroid coordinates were then calculated for each species within each shape space. This data was used as the input for a hierarchical clustering that produced dendrograms illustrating morphological similarity of the species based on the outline shape of a given tooth position. The nine deriving dendrograms were then combined into a single majority consensus tree using the *ape* package (Paradis & Schliep 2019) within the *R v.3.5.2.* programming environment (R Core Team 2013).

To visualise the ideal contour of an ordinary member within a group, a consensus shape can be calculated for any subset of specimens by repeating the generalised Procrustes superimposition on the individuals belonging to the selection and averaging the subsequent fitted coordinates of the corresponding LMs and SLMs (see e.g. the consensus representations for every tooth position of *S. citelloides* on Fig. 2).

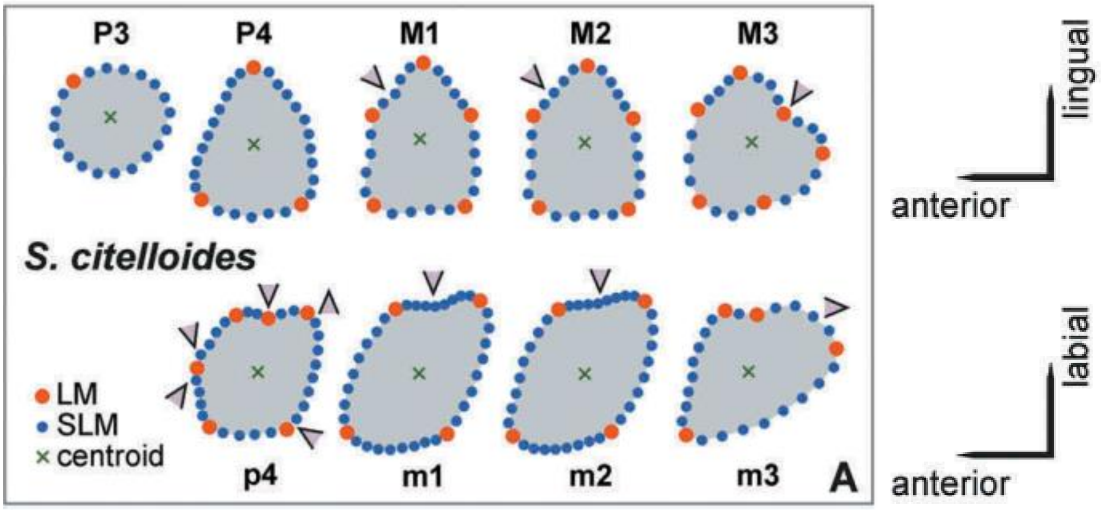

Figure 2. *Consensual occlusal outlines represented by landmarks (LMs) and semilandmarks (SLMs) of different right S. citelloides premolars and molars. The arrows are indicating diagnostic differences between S. citelloides and its once supposed descendant, S. citellus.*

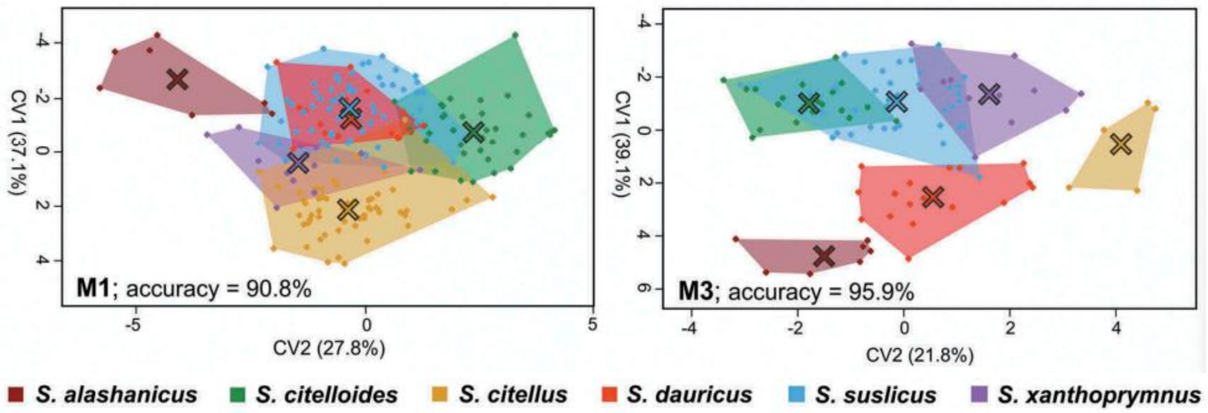

Figure 3. *Ordinations resulting from canonical variate analysis (CVA) of landmark configurations in the example of the upper first (M1) and third molars (M3). Group centroids are marked with crosses.*

The following main conclusions were drawn based on the above described GM analysis: **1)** The convex hulls of the studied species have similar areas to each other on all ordinations, which means that the morphological variability of *S. citelloides* teeth is comparable to that of the extant ground squirrels of the same genus. **2)** Although there are overlaps between some of the convex hulls, when considering all tooth positions, *S. citelloides* clearly forms a distinct group that cannot be merged with any of the studied species, thus it can be considered a valid taxon. **3)** Apart from the case of M1 and P3, the hierarchical clustering always found that the teeth of *S. citelloides* are most similar to *S. suslicus*. Due to the low sample number and the lack of landmarks on the outline, results related to P3 should be taken with caution. The outline shape of the M1 of *S. suslicus* turned out to be more similar to that of *S. dauricus* than *S. citelloides*. By combining the dendrograms, the only group that remained certain was the *S. citelloides – S. suslicus* clade with the support of seven individual trees out of the nine. This agrees well with the results of the standard phylogenetic analysis, further strengthening the idea that

S. citelloides has in fact closer affinities for *S. suslicus* rather than *S. citellus* as implied by the species name and as viewed by some researchers (e.g. Kryštufek & Vohralík 2005). **4)** Using the consensus shapes produced during the GM analysis, subtle but diagnostic differences were recognised that can help researchers to differentiate *S. citelloides* from other, morphologically similar taxa. These are indicated by arrows on Fig. 2. As an example, the facial side of the lower first (m1) and second molars (m2) in occlusal view are more concave compared to *S. citellus*.

To sum up, this subproject provided key information regarding the original aim of our research. It turned out that outline analysis using a GM methodology is indeed applicable to relatively simplistic tooth contours. The major hinderance in our approach was that the first step of the digitisation was done manually, which was a tedious and time-consuming process. The contours were recorded directly from optical micrographs, which typically have a shallow depth of field. On such images, the lateral sides of the teeth, which surround the occlusal surface, are gradually becoming less focused as we move away from our area of interest. This condition prevents automated edge detection with a level of precision that is necessary for further analysis. However, defining the entire outline rather than placing LMs and SLMs directly onto the images allowed us to identify crucial points via an automated approach that eliminated the subjectivity of pinpointing inflexions based solely on the judgement of an investigator. Such algorithmic approaches increase the reproducibility of the results and improve the comparability of GM studies performed by different researchers. Our results also pointed out that the outline analysis of the teeth can indeed provide valuable information that can be utilised in taxonomic research. With this approach, the variability of a contour can be evaluated and compared with other taxa, the average shape of a group can be visualised, and similarities with, as well as differences from other forms can be identified objectively. As an independent tool, the GM methodology also provided limited insight in the phylogeny of ground squirrels.

The subproject was outlined in 2018 during the European Ground Squirrel Meeting (EGSM; Virág & Pazonyi 2018), and its results were presented to the scientific community during 2019 at an INQUA workshop held in the Charles University of Prague (connected to their HABCOM 1606P project: Ground Squirrels on the March - Expansion and Speciation in the Quaternary of the Circum-Pontic Area and Surroundings; see Popova et al. 2021 for details), at the GEOMATES international conference (Pazonyi & Virág 2019a), and also at the Annual Meeting of the Hungarian Palaeontologists (Pazonyi & Virág 2019b). The conclusive article was published in *Historical Biology* (Sinitsa et al. 2021; published online: 2019, https://doi.org/10.1080/08912963.2019.1677640, Q1, IF: 1.942).

Voles and lemmings (Rodentia: Cricetidae: Arvicolinae) have very distinctive, intricately folded molar enamel which encapsulates the dentine core of a tooth. The mesial end of a first lower molar is named the anterior cap (AC), whereas the posterior loop is called the talonid. The cap is divided from the rest of the tooth by the so called neck. The alternating indentations (or re-entrant angles) of the enamel on both sides of the teeth separate the triangles (Ts, or salient angles). These are labelled from distal to mesial direction, thus the hindmost triangle on the lingual side is termed T1. The AC together with all triangles in front of T3 are referred as the anteroconid-complex (ACC). In the case of several separate arvicolid lineages, new triangles emerged evolutionary at the mesial end of the lower first molars with the gradual infolding of the AC. This made their food processing more efficient via increasing the number of orofacially oriented cutting edges, which interacted with those of the upper teeth during the proal jaw motions (i.e. when the mandible moves rostrally while in occlusion). Hence, the outline of the lower first molars of arvicolids varies from species to species. As a part of the NKFIH FK128741 project, we aimed to distinguish taxa by the means of a GM analysis.

For this subproject, a total of 706 lemming teeth belonging to nine, and 4727 vole teeth (including recent material) assignable to ten different species were photographed and digitised in occlusal view (Tab. 2).

Table 2. *Specimens involved in the geometric morphometric analysis of arvicolids.*

lemmings	**m1**	**voles**	**m1**
Borsodia newtoni	64	***Agricola agrestis***	350
Borsodia petenyii	273	***Alexandromys oeconomus***	443
Lagurodon arankae	79	***Microtus (Allophaiomys) pliocaenicus***	723
Lagurus lagurus	2	***Microtus (Allophaiomys) praehintoni***	9
Prolagurus pannonicus	22	***Microtus (Microtus) arvalis***	623
Villanyia eleonorae	205	***Microtus (Microtus) nivalinus***	177
Villanyia exilis	15	***Microtus (Microtus) nivaloides***	587
Villanyia klochnevi	29	***Microtus (Terricola) arvalidens***	855
Villanyia laguriformes	17	***Microtus (Terricola) hintoni***	339
		Microtus (Terricola) subterraneus	621
TOTAL	706	**TOTAL**	4727

Likewise, in the case of ground squirrels, following a manual digitisation step, the occlusal contours were rarefied to 100 equidistant points using the same function as before. Orientational differences were removed by rotating the specimens around their centroid until the longer edges of their minimum area bounding rectangle became parallel to the y-axis of an arbitrarily defined Cartesian coordinate system. Rather than expressing the shapes as a function of their centroids, we described the outlines as a series of the consecutive x-coordinates during the next step. Zero-crossings of the first-order derivative of the resulting curve correspond to the tips of the salient angles and the deepest points of the re-entrant angles (Fig. 4; see also Potočnik 2015).

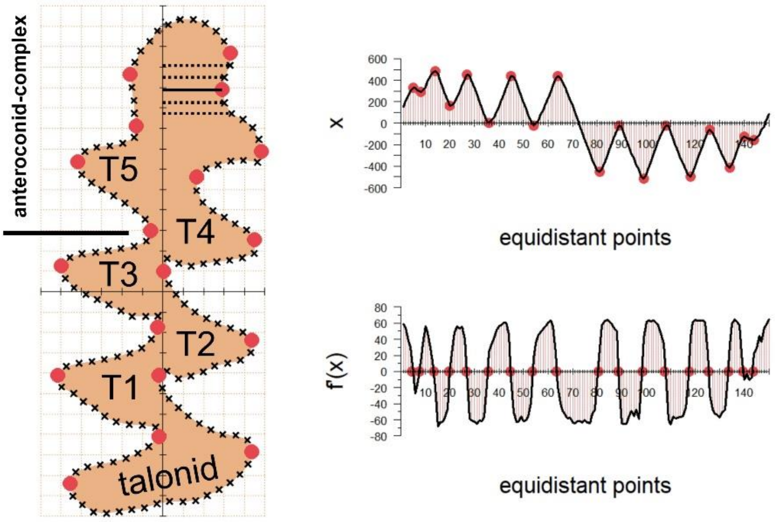

Figure 4. *Automated point detection demonstrated in the case of a Lagurodon arankae lower first molar. LMs were placed where the first order derivative of the consecutive x-coordinates changes sign.*

Since this GM analysis relies on placing an equal number of LMs over different morphologies, points that were identified over such curvature extrema, which are not traceable on all studied outlines, were removed after the automated detection step. For voles, this meant that only the 14 distal LMs were kept, but the mesial points of the ACC were deleted. In addition, two shape descriptors (the one with the highest and the other with the lowest y-coordinate) were also selected. As in the previous subproject, the residual morphology of the original contours was described by putting SLMs onto the segments between the LMs (see on Fig. 5). Lemmings were approached with a more simplified point placement strategy visible on Fig. 6. The obtained configurations were then fed into a CVA following a generalised Procrustes superimposition. To aid the interpretation of the arising ordinations (Figs. 5 and 6), consensus shapes were also generated for each of the studied species.

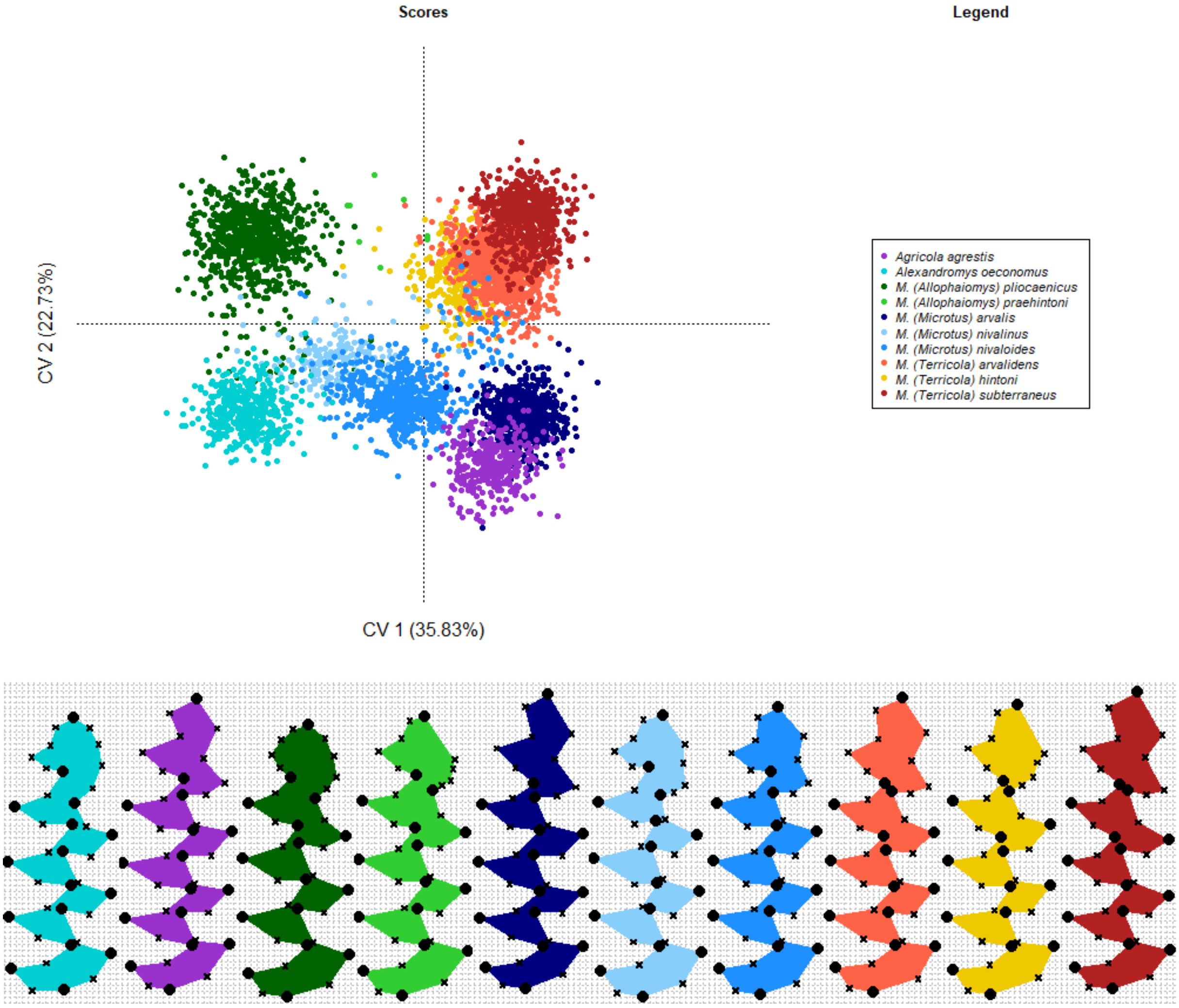

Figure 5. *Ordination resulting from canonical variate analysis (CVA) of vole lower first molars. Consensus shapes for groups with matching colours are shown below. Abbreviations: M.: Microtus.*

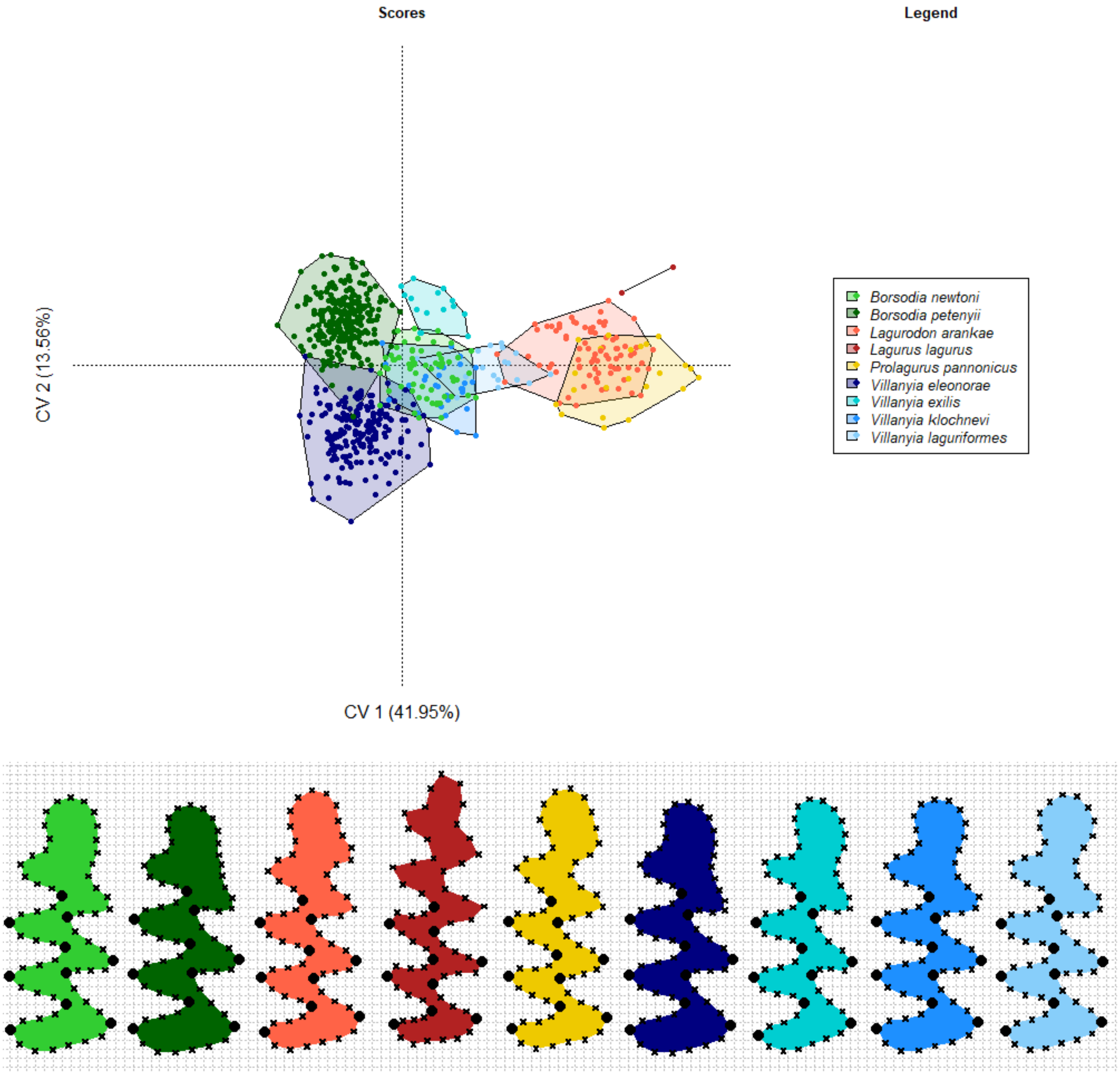

Figure 6. *Ordination resulting from canonical variate analysis (CVA) of lemming lower first molars. Consensus shapes for groups with matching colours are shown below.*

The above discussed GM methodology separated the studied vole and lemming species quite efficiently. It also allowed us to reconstruct evolutionary lineages within the respective larger clades, which is demonstrated here by listing our major findings obtained through studying vole teeth: **1)** Species plotting on the positive side of the second PC axis on Fig. 5 have a so called "Pitymys rhombus", which means that their buccal T4 and lingual T5 triangles are not sufficiently isolated, but merge into a rhombus-shaped area just behind the cap. Compared to the rootless molars of the derived *Microtus* (*Microtus*) voles, this represents a plesiomorphic state. **2)** It is visible on Fig. 5 that more advanced, elongated teeth with a well-developed ACC and a higher triangle count are located further towards the positive end of the first PC axis. To a lesser degree, this is also true to the ordination based on lemming teeth, depicted on Fig. 6. **3)** By tracing slight morphological changes from group to group, two evolutionary lineages seem plausible among the voles (these span from green to red and from green to dark blue on Fig. 5. **a)** One leads from *M*. (*Allophaiomys*) *pliocaenicus* through *M*. (*A*.) *praehintoni* towards the *M*. (*Terricola*) group. The most basal member of the latter is *M*. (*T*.) *hintoni*, while a fourth re-entrant angle appears as an apomorphy at the buccal side of the cap in the case of *M.* (*T.*) *arvalidens* and *M.* (*T.*) *subterraneus*. **b)** The other also starts with *M.* (*A.*) *pliocaenicus*, but leads through *M.* (*M.*) *nivalinus* and *M.* (*M.*) *nivaloides*, until it ends in *M.* (*M.*) *arvalis*. These ideas are supported by the first and last appearance dates of the mentioned taxa and are in quite good agreement with the assumptions of Maul & Markova (2007). However, the recent study of Abramson et al. (2021) estimated surprisingly old divergence times for several arvicoline genera using mitogenomic data. It has to be mentioned too that *Alexandromys oeconomus* and *Agricola agrestis*, while strikingly similar to some of the mentioned species, represent arvicolines that branched out earlier within this clade than microtids.

To sum up, the results of the second subproject showed that the outline analysis of teeth can provide valuable phylogenetic information in a much larger extent than it was indicated by the first study. Partial results related to this work were presented in 2019 at the GEOMATES international conference (Virág et al. 2019a) and during the next year at the Annual Meeting of the Hungarian Palaeontologists (Pazonyi et al. 2020). The progress leading to a conclusive article was slow due to the fact that prior to the beginning of this project we already proved the applicability of a similar but less automated LM-based GM methodology using a more restrictive comparative dataset (see Pazonyi et al. 2018, https://doi.org/10.1016/j.quaint.2017.07.019, Q1, IF: 1.952). And so, during the runtime of the project, our attention shifted rather towards those subprojects through which we hoped that we would be able to solve such issues, which prevented us in developing a more flexible approach suitable for a wide variety of morphologies. As of now, a manuscript containing the new results on voles is in the final steps of its preparation for the journal *Historical Biology*. Although it is not yet submitted, this study was of key importance, for it helped us to realise that the methodology discussed so far always needs adjustments and optimisation if used on at least moderately different morphologies. Heavily relying on SLMs weakens the discriminatory power of the analysis, hence, it is not an optimal solution for the latter issue. Consequently, we started to seek alternatives in order to establish a universally applicable protocol.

Procapreolus loczyi (Artiodactyla: Cervidae: Capreolinae) was introduced by Pohlig as *Cervus* (*Paleaxis*) *loczyi* based on some fragmentary antlers originally assigned to *Pliocervus matheroni* from Polgárdi, Fonyód, Karád, and Baltavár. Its description was published by Kadič (1911) as a Hungarian mirror translation. During the same year, Kormos (1911) appointed additional material from Polgárdi, including cranial elements with teeth to the same taxon. However, he believed that instead of the spotted deer, this species was more closely related to the extant roe deer (*Capreolus capreolus*). The phylogenetic relationships and the validity of *P. loczyi* is under debate up until today. Croitor (2014, 2018), for example, argued that the antlers figured in the original description lack diagnostic characters due to their poor preservation and most likely belong to different taxa. As a part of the NKFIH FK128741 project, we intended to shed some light to the aforementioned issues by the means of a GM analysis on the occlusal outline of the selenodont cervid premolars and molars.

Unfortunately, the data acquisition was hindered by the COVID19 pandemic, during which the main Hungarian fossil collections (especially the one housed by the Supervisory Authority for Regulatory Affairs of Hungary) were inaccessible, and visiting foreign institutions (such as the Natural History Museum in Vienna) was also impeded. Although, the fixed-term contract of co-investigator Bence Szabó was prolonged, the money reallocated from the traveling budget was only enough to cover the expenses of a part-time status. Thus, the progress of this subproject slowed down and during his application period, Bence Szabó was not able to collect a comparative material that is large enough to allow us drawing statistically significant conclusions regarding the above listed issues. This became rather obvious during the data analysis and the preparation of a manuscript.

During the disrupted period, we used some already available specimens for a study, in which we explored the possibility of separating species and tooth positions using the random forest machine learning algorithm. We planned to apply this approach later as an independent control of the GM classification. The results of the analysis were presented to the scientific community in 2019, during the GEOMATES international conference (Szabó & Virág 2019a). We also utilised a landmark based approach (similar to those described above) to facilitate the reliable identification of the position of isolated reindeer (*Rangifer tarandus*) teeth from Ságvár. The outcomes were presented during the Annual Meeting of the Hungarian Palaeontologists (Szabó & Virág 2019b). Albeit a definitive article on the questions related to *P. loczyi* was not published yet, the subproject is already in a rather developed state, and by the inclusion of new comparative material, we aim to complete it in the foreseeable future. Nonetheless, the preliminary outcomes proved to be vital in pushing our research further towards the originally planned end result, thus we give here a brief summary of what we achieved so far.

For this subproject, we studied premolars and molars from the type localities of *P. loczyi* (Polgárdi and Baltavár) supplemented with additional material referred to the same species (e.g., Braşov), and comparative specimens belonging to different taxa (including *Capreolus sussenboernensis* from Tarkő an Gombasek and recent *C. capreolus*; Tab. 3).

Table 3. *Specimens involved in the geometric morphometric analysis of cervids.*

-	specimens	teeth	p2	p3	p4	m1	m2	m3	P2	P3	P4	M1	M2	M3
C. capr.	72	249	24	34	25	16	19	17	5	4	5	24	35	41
C. suess.	7	7	0	1	1	1	1	1	0	0	1	0	1	0
C. sp.	19	22	0	0	0	0	4	1	1	3	1	2	4	6
P. loczyi	59	59	0	6	6	2	3	11	0	0	1	9	9	12
TOTAL	157	337	24	41	32	19	27	30	6	7	8	35	49	59

The occlusal outline of cervid teeth can differ extensively from position to position and changes radically with tooth wear (Fig. 7). In order to eliminate wear related variance, only individuals, which can be categorised into the late IDAS2 stage of Anders et al. (2011), were used in the comparison. The position related issue can be solved by using predominantly equidistant SLMs (as we did in Szabó & Virág 2019b), but they are subpar compared to anatomically or geometrically defined points.

We realised that by using forward complex discrete Fourier transformation (DFT), any closed contour described by a set of 2D coordinates (such as a digitised tooth outline) can be decomposed to a sum of circular motions with harmonic frequencies called epicycles or rotating phasors (Kuhl & Giardina 1982, Haines & Crampton 2000, Godefroy et al.2012). The number of the resulting epicycles is identical with the number of the points in the original outline. The characteristics of each epicycle (i.e. its amplitude and starting phase angle) are defined by two coefficients often referred as Fourier descriptors (FDs). The methodology provides an ideal alternative to the LM-based analysis by eliminating the problem of finding an equal number of prominent points on different morphologies.

As in the previous subprojects, the manually placed outline descriptors were rarefied to 100 equidistant points. The FDs were then calculated using equation 31.6 of Smith (2002). The amplitude and phase of an epicycle was determined by substituting its FDs into equation 8.6 of Smith (2002). An initial outline can be synthesised via superimposing the resulting epicycles in a decreasing order of amplitude (where each new one is centred around the endpoint of the previous phasor). The first two epicycles (defined by four FDs) describe an ellipse, the major axis of which coincides with the axis of elongation of the original shape. By the addition of more epicycles, the produced contour will gradually converge towards the actual outline (Fig. 8).

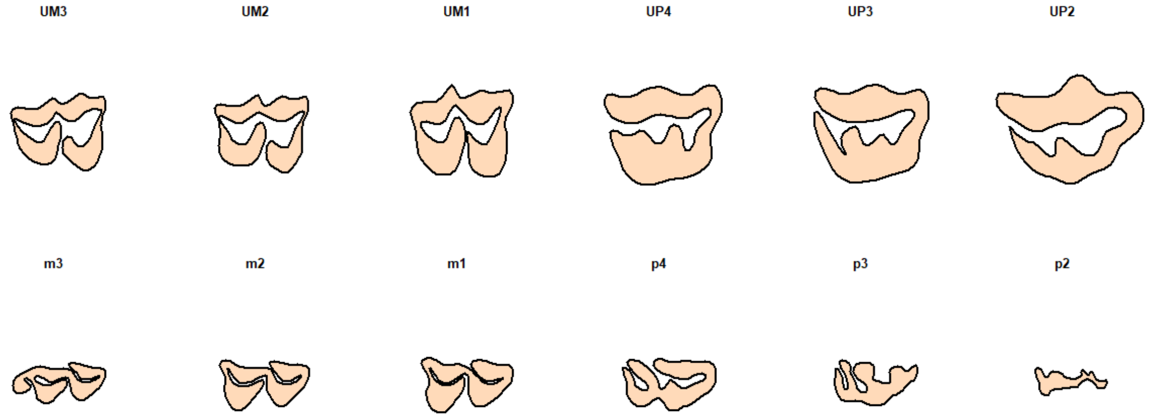

Figure 7. *The positional variation of the occlusal relief in the case of C. capreolus. Abbreviations: m: lower molar, p: lower premolar, UM: upper molar, UP: upper premolar.*

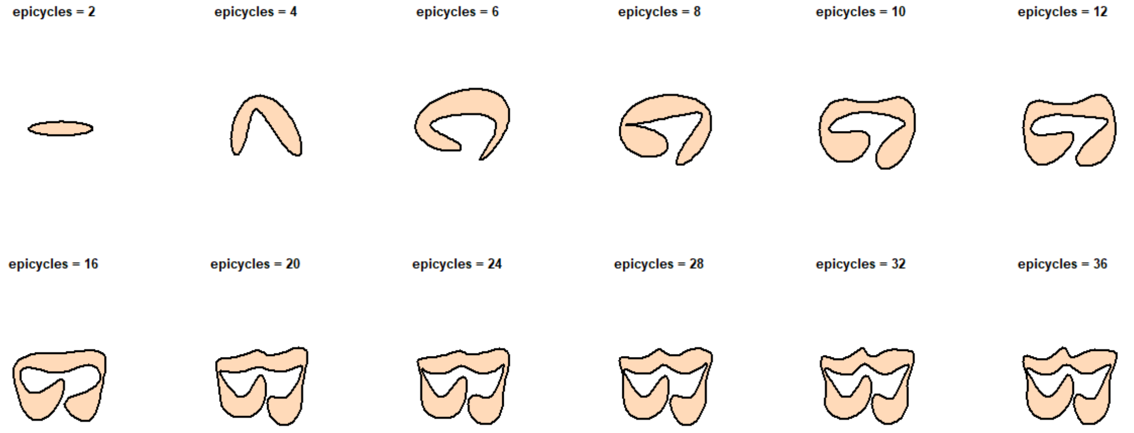

Figure 8. *Via the superimposition of epicycles resulting from the DFT of shape descriptors, original contours can be smoothed to a desired degree. The more epicycles are used, the better the approximation will be, which is demonstrated in the case of an upper second molar of a C. capreolus.*

This inverse DFT approach allows the smoothing of shapes with varying degrees by summing only the first epicycles. In order to use FDs for the purpose of contour comparison, they must be made independent of the size and the orientation of the original outline, as well as the starting point of the last phasor on the contour. This normalisation was based on the above mentioned first ellipse as a reference. Following the steps described by Kuhl & Giardina (1982) and Godefroy et al. (2012), the FDs were rescaled so that the major axis of the first ellipse (i.e. the sum of the amplitudes of the first two epicycles) became equal to one. The centred outlines were rotated until the minor and major axes coincided with the horizontal and vertical axes of the underlying Cartesian coordinate system. The FDs were also corrected so that the starting phase angle of the first two epicycles became zero. The resulting Fourier coefficients were used as variables in a principal component analysis (PCA) implemented by the *prcomp()* function of the built-in *stats* package of *R*. The first 40 pairs of FDs were considered for this analysis to provide a good balance between a satisfying description of the occlusal shape, and an efficient filtering of measurement noise without using an excessive number of epicycles. Some of the deriving ordinations are depicted on Figs. 9 and 10.

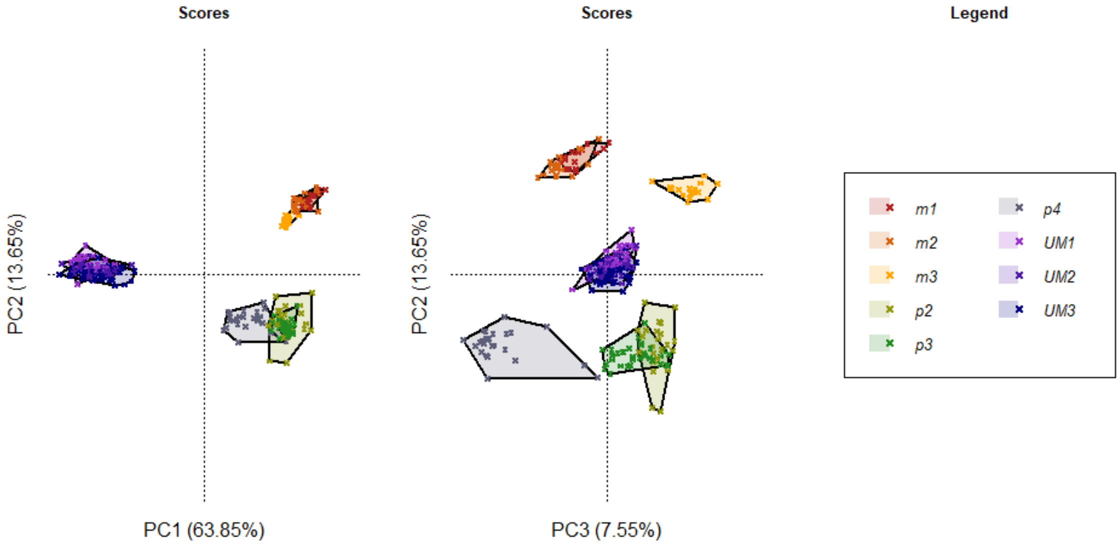

Figure 9. *Ordination resulting from principal component analysis (PCA) of cervid teeth. Abbreviations: m: lower molar, p: lower premolar, UM: upper molar.*

The above described GM analysis resulted in the following outcomes: **1)** The DFT method was able to adequately separate different tooth positions from each other (Fig. 9), which can be useful, especially when dealing with isolated premolars and molars. **2)** The comparison of teeth of the same position with each other suggest that the occlusal morphology of *P. loczyi* is indeed somewhat different from other taxa. This is especially true in the case of the upper second molars (Fig. 10). However, due to the small sample and the lack of contemporary comparative taxa, this statement is not conclusive enough yet. **3)** By averaging the outlines produced by the inverse DFT approach, consensus shapes were produced for each tooth position of each species, which helped us to identify diagnostic differences between the analysed taxa. For example, *P. loczyi* has an orofacially compressed upper second molar, the palatinal contour of which have marked concavities near both the paracone and the metacone. However, this latter feature is less striking than in the case of *C. suessenbornensis*.

This study showed that elliptical Fourier analysis is a robust alternative to the LM based approach. Moreover, it has the advantage that it can be applied to any closed contour (or open curve) with ease. The last question yet to be answered was if the grouping capabilities of the DFT method are comparable with that of the original LM-based approach. This we intended to answer during the fourth subproject.

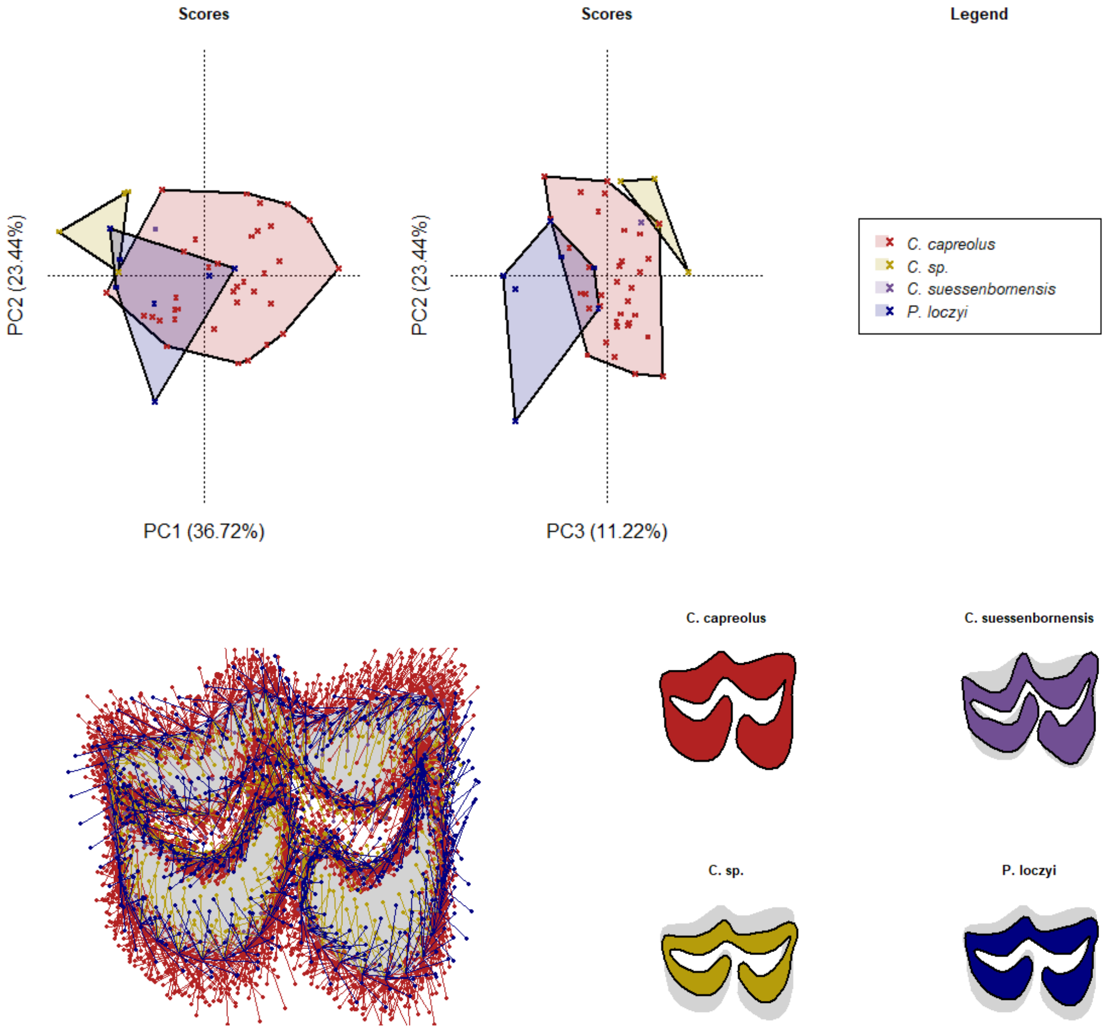

Figure 10. *Ordination resulting from principal component analysis (PCA) of the upper second molars of C. capreolus, C. suessenbornensis and P. loczyi. The differences between the groups are visualised below the plot. The grey shaded area represents the consensus of the entire sample.*

Conodonts are the teeth-like phosphatic elements of extinct eel-like jawless vertebrates. Their abundance, rapid evolution combined with their high preservation potential make them one of the most widely used microfossils in applied geosciences. Their primary application field is the relative dating of marine rocks, predominantly of basin facies. P1 elements (Fig. 11A-C) in particular express extensive and obvious morphological change during the evolution of the group. An accurate biostratigraphical application can only be based on a thorough and steady taxonomical framework. Primarily, taxa diagnoses are based on qualitative criteria. However, the subjective definition of the morphological features induces differing taxonomical concepts among individual researchers that may cause biases in stratigraphic subdivision. We believe that such issues can be improved by studying the intra- and interspecific variability of species by the means of objective GM methods.

Norian (Upper Triassic) biostratigraphy, for example, is hampered by several taxonomical issues that mainly derive from the overly general original diagnoses and/or the sparse illustration of the species characteristic for this age (Karádi 2018a). Descriptions of species rarely include detailed comparison with other taxa from the same time interval, therefore many specimens with potentially transitional characters either fit in more than one species or do not fully fit in any established species, which results in taxonomic and stratigraphic ambiguities. As a part of the NKFIH FK128741 project, we aimed to test whether GM methodologies can reveal such morphological relationships that are, at first glance, not so obvious when working with conodont elements solely from a qualitative point of view, and thus improve taxonomic subdivisions.

For this subproject, we studied a total of 136 lower Norian conodont P1 elements. Of the specimens considered, 80% were unambiguously assigned to the taxa *Ancyrogondolella quadrata*, *A. rigoi*, *A. triangularis*, *A. uniformis*, and *Metapolygnathus mazzai*. For specimens bearing morphological characters not fully fitting the original diagnoses of these species, the open nomenclatural term *ex gr.* (of the group) was used. Holotypes of the listed species were also included in the study based on the best illustrations available in the literature (listed in Tab. 4). Only undeformed, complete, adult (GS4–GS6; based on the ontogenetic series defined in Mazza & Martínez-Pérez 2015) specimens were involved in the present study.

Table 4. *Specimens involved in the geometric morphometric analysis of conodonts.*

-	specimens	ex.gr.	reference for image of holotype
Ancyrogondolella quadrata	35	12	Orchard 1991
Ancyrogondolella rigoi	42	8	Noyan & Vrielynck 2000
Ancyrogondolella triangularis	15	0	Budurov 1977
Ancyrogondolella uniformis	12	2	Orchard 1991
Metapolygnathus mazzai	6	4	Mazza et al. 2012
TOTAL	110	26	

We chose to analyse the element (Figs. 11D and 11F) and the keel outlines (Figs. 11E and 11G) which both bear taxon specific features. As in the previous subprojects, the manually digitised outlines were rarefied to 100 equidistant points within the *R v.4.1.2.* programming environment (R Core Team 2013). From this point forward, the analysis continued in two separate directions: **a)** We marked the position of the cusp and the pit as anatomical landmarks, as their locations are key diagnostic traits. Geometrical landmarks were selected on the outlines using automated algorithms that searched for the sharpest inward facing angle between neighbouring shape descriptors of a specific region. On the element outline, the anterior end and the posterolateral corners were marked. On the keel outline, the anterior end and the two posterior tips (if the keel was bifid) or the posterolateral corners (if the keel was non-bifid) were selected. The sections between the LMs were resampled by six equidistant SLMs on the posterior margin and twelve on each lateral margin (Fig. 11D-E). These numbers were chosen so that the points have a similar density on all margins in the case of most studied specimens. Following the exact same generalised Procrustes superimposition that was described earlier, the resulting coordinates formed the basis of a PCA. **b)** The aforementioned 100 equidistant points were also used in an elliptical Fourier analysis, which followed identical steps as described in the case of the cervid teeth. The first 20 pairs of the normalised FDs were deemed sufficient for describing the outlines (Fig. 11F-G), thus they were also used to produce PCA ordinations.

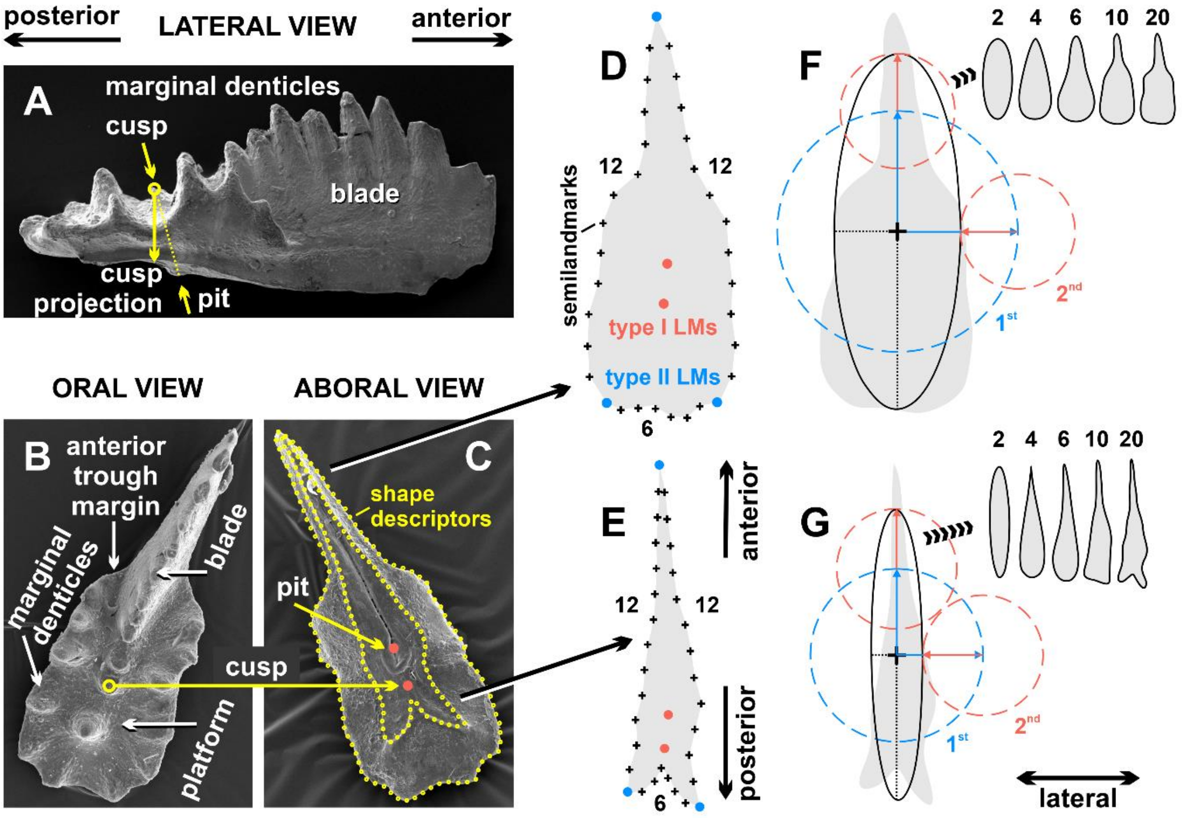

Figure 11. *A. uniformis P1 element in lateral (**A**), oral (**B**) and aboral (**C**) view. The 100 equidistant shape descriptors are depicted on **C**, whereas the landmark configurations are shown on **D** and **E**. Via the superimposition of epicycles resulting from the DFT of shape descriptors, the original contours can be smoothed to a desired degree. The more epicycles are used, the better the approximation will be (**F**, **G**).*

The GM analysis led to the following conclusions: **1)** Both the LM and the FD-based GM approaches were able to distinguish P1 elements of different conodont taxa based on their aboral outline and keel contour, leading to essentially identical ordinations (Fig. 12). This means that the DFT methodology proved to be an equally efficient alternative as the initially used LM analysis. **2)** The species were better separated based on their keel contours than their element outlines. **3)** Each FD-based PCA ordination resulted in basically the same group structure if it included at least the first four coefficient pairs. Raising the number of the used FDs barely improved the discrimination. This means that general shape differences are responsible for the visible grouping, whereas finer details of the contours are not as influential. **4)** *A. rigoi* has a central position, partially overlapping with the convex hulls of all studied taxa. However, with the exception of *A. quadrata*, it can be differentiated from the others by traits that are not visible on the outline. These two species together vary on a great range with a plethora of transitional morphologies that hinders their secure distinction. Although the merging of the two groups seems plausible, their combined shape variance is unrealistically large compared to the reliably separable coexisting forms. **5)** Mathematically produced consensus morphologies allowed us to objectively describe the typical outline of each species focusing especially on traits, which help their differentiation from each other. For example, *M mazzai* is slender, having a rectangular platform with subparallel margins. The anterior platform termination is abrupt. The pit is located clearly anterior to the mid-length of the platform. The keel shows a moderate posterior bifurcation that develops relatively far behind the pit. **6)** Our results showed that taxonomists often choose specimens with clearly distinct morphologies, or even atypical end-members in an assemblage for holotypes. For example, the holotype of *M. mazzai* is located in a peripheral position within the convex hull of its own species, relatively far from the group centroid (Fig. 12). Compared with the consensus shape, it has a markedly longer platform and a slightly more asymmetric appearance (Fig. 13). We believe that prior to the holotype designation and the making of the species diagnosis, more emphasis should be placed in the future on exposing the intraspecific variability by objective GM methods.

This subproject was outlined in 2019 during the STRATI international conference (Virág et al. 2019b), and its results were presented to the scientific community in 2022 at the European Conodont Symposium (ECOS; Virág & Karádi 2022). The conclusive article was published in *Palaeontology* (Virág & Karádi 2023, https://doi.org/10.1111/pala.12649, D1, IF: 3.547).

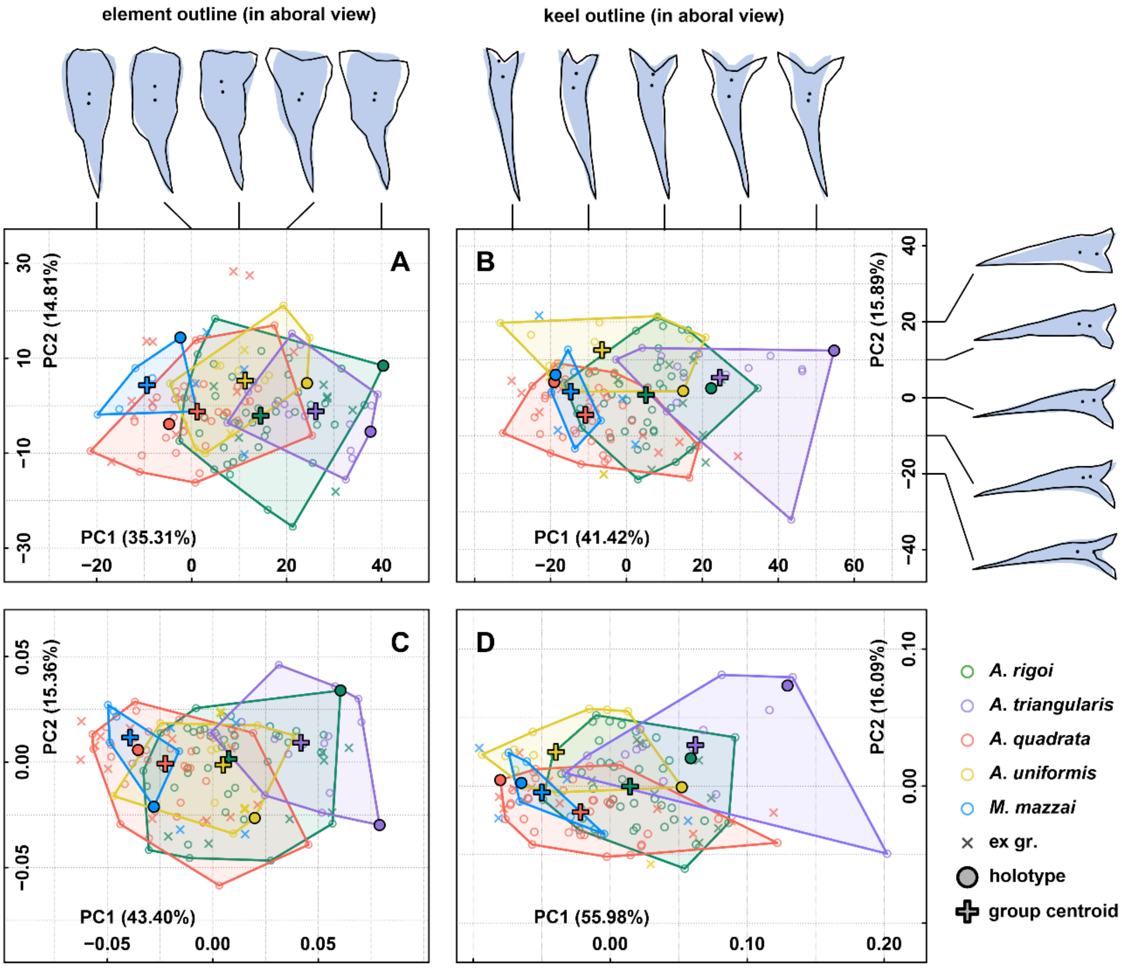

Figure 12. *Ordinations resulting from principal component analysis (PCA) of conodont elements.* ***A*** *and* ***B*** *were based on LM configurations, whereas* ***C*** *and* ***D*** *were produced using the first 20 pairs of FDs. Shape changes along the axes are shown for the element outline on* ***A*** *and for the keel on* ***B*** *by black contours. The grey shaded silhouettes represent the consensus morphology for all studied specimens.*

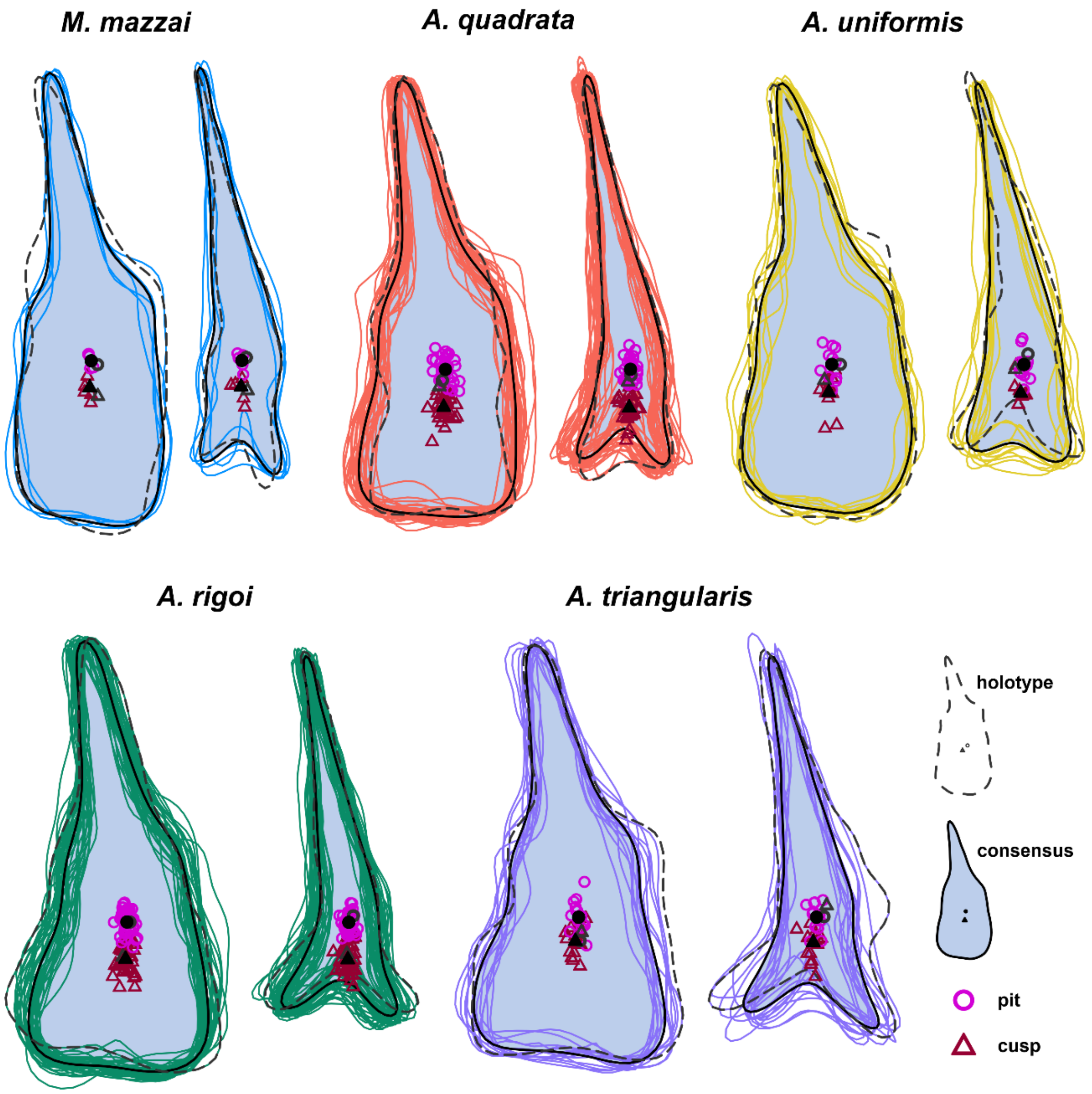

Figure 13. *Mathematically produced consensus shapes of the analysed species (black contours) projected over the outlines of other specimens assigned to the respective groups. Holotypes are highlighted with dashed lines.*

Based on the above discussed examples, we believe that the main aim of the NKFIH FK128741 project, which was to develop and test a geometric morphometric methodology that can be applied on various tooth outlines, was successfully achieved. After experimenting with a landmark-based approach, we decided to use discrete Fourier transformation (DFT) on the contours instead, for achieving the same results. We demonstrated the usefulness of both procedures in solving taxonomy related issues and in tracing phylogenetic lineages. In order to ensure a reproducible and readily applicable protocol, we automated most steps of the landmark acquisition. The custom *dft()* function that returns the Fourier descriptors of a set of shape coordinates, the *normDft()* function that performs the normalisation of the resulting FDs, and the *invDft()* function that synthesises an outline from a set of FDs using an adjustable number of epicycles are available as part of the supplementary material for

Virág & Karádi (2023; https://doi.org/10.5281/zenodo.7659056), and also from a version-tracked, open-access GitHub repository (https://github.com/paleoscript/DFT). All of these were written in the *R* programming environment. Besides the computer-assisted point acquisition and contour description, we started to experiment with automated edge detection too during the project (see Virág & Szabó 2019). We developed a user-friendly utility software that performs the latter task on images with sufficiently high resolution and contrast, and made it freely available online (http://geode.hu/_USERS/Zircon.html). In addition, the software allows the Fourier smoothing of outlines and saving some frequently used shape parameters.

We expect that our methodology will help researchers to eliminate subjectivity from shape analysis, which is a long-standing intention of biologists and palaeontologists working in the field of taxonomy. We also think that through the exploration of shape variability and the characterisation of the typical representative of an assemblage, the process of describing new species and designating their type material would also benefit from a contour analysis with the protocol developed here. Furthermore, the DFT methodology is flexible enough to be able to be easily applied to not only tooth outlines, but to any shape. Thus, we hope that the functions and utilities developed during this project combined with the methodology discussed above will aid many researches of various kinds in the future.

The most important outcomes of the NKFIH FK128741 project will be summarised on the 17th of November during a plenary session on the *Most recent advances of vertebrate palaeontology* in Hungary organised by the Hungarian Academy of Sciences in the framework of the annual Hungarian Science Festival.

References

Abramson, N.I., Bodrov, S.Y., Bondareva, O.V., Genelt-Yanovskiy, E.A. & Petrova T.V. (2021): A mitochondrial genome phylogeny of voles and lemmings (Rodentia: Arvicolinae): Evolutionary and taxonomic implications. *PLoS One 16(11), e0248198.*

Anders, U., Koenigswald, W. von, Ruf, I. & Smith, B.H. (2011): Generalized individual dental age stages for fossil and extant placental mammals. *Paläontologische Zeitschrift 85(3), pp. 321-339.*

Budurov, K.J. (1977): Revision of the Late Triassic platform conodonts. *Geologica Balcanica 7, pp. 31-48.*

Croitor, R. (2014): Deer from Late Miocene to Pleistocene of Western Palearctic: matching fossil record and molecular phylogeny data. *Zitteliana B 32, pp. 115-153.*

Croitor, R. (2018): Plio-Pleistocene Deer of Western Palearctic: Taxonomy, Systematics, Phylogeny. *Institute of Zoology of the Academy of Sciences of Moldova, Chişinău, p. 140.*

Ermakov, O.A., Simonov, E., Surin, V.L., Titov, S.V., Brandler, O.V., Ivanova, N.V. & Borisenko, A.V. (2015): Implications of hybridization, NUMTs, and overlooked diversity for DNA barcoding of Eurasian ground squirrels. *PLoS One 10(4), e0120631.*

Godefroy, J.E., Bornert, F., Gros, C.I. & Constantinesco, A. (2012): Elliptical Fourier descriptors for contours in three dimensions: a new tool for morphometrical analysis in biology. *Comptes Rendus Biologies 335, pp. 205-213.*

Haines, A.J. & Crampton, J.S. (2000): Improvements to the method of Fourier shape analysis as applied in morphometric studies. *Palaeontology 43, pp. 765-783.*

Harrison, R.G., Bogdanowicz, S.M., Hoffmann, R.S., Yensen, E. & Sherman, P.W. (2003): Phylogeny and Evolutionary History of the Ground Squirrels (Rodentia: Marmotinae). *Journal of Mammalian Evolution 10, pp. 249-276.*

Herron, M.D., Castoe, T.A. & Parkinson, C.L. (2004): Sciurid phylogeny and the paraphyly of Holarctic ground squirrels (*Spermophilus*). *Molecular Phylogenetics and Evolution. 31, pp.1015-1030.*

Kadič, O. (1911): A Balaton vidékének fosszilis emlősmaradványai. *pp. 1-24. In: A Balaton tudományos tanulmányozásának eredményei I. kötet - A Balatonnak és környékének fizikai földrajza. 1. rész: A Balaton környékének földrajzi leírása, orografiája és geologiája. Függelék: A Balatonmellék palaeontológiája IV.kötet, Magyar Földrajzi Társaság Balaton-Bizottsága. Budapest, p. 710.*

Karádi, V. (2018): Middle Norian conodonts from the Buda Hills, Hungary: an exceptional record from the Western Tethys. *Journal of Iberian Geology 44, pp. 155-174.*

Kormos, T. (1911): A polgárdi pliocén csontlelet. *Földtani Közlöny 41, pp. 48-64.*

Kormos, T. (1915): A pilisszántói kőfülke emlősei, rendszertani, zoogeográfiai és származástani tekintetben. *A Magyar Királyi Földtani Intézet Évkönyve. 23(6), pp. 340-431.*

Kryštufek, B. & Vohralík, V. (2005): Mammals of Turkey and Cyprus. Rodentia I: Sciuridae, Dipodidae, Gliridae, Arvicolinae. *Koper, Science and Research Centre of the Republic of Slovenia, p. 298.*

Kuhl, F.P. & Giardina, C.R. (1982): Elliptic Fourier features of a closed contour. *Computer Graphics & Image Processing 18, pp. 236-258.*

Maul, L.C. & Markova, A.K. (2007): Similarity and regional differences in Quaternary arvicolid evolution in Central and Eastern Europe. *Quaternary International 160, pp. 81-99.*

Mazza, M. & Martínez-Pérez, C. (2015): Unravelling conodont (Conodonta) ontogenetic processes in the Late Triassic through growth series reconstructions and X-ray microtomography. *Bollettino della Societa Paleontologica Italiana 54, pp. 161-186.*

Mazza, M., Rigo, M. & Gullo, M. (2012): Taxonomy and biostratigraphic record of the Upper Triassic conodonts of the Pizzo Mondello section (western Sicily, Italy), GSSP candidate for the base of the Norian. *Rivista Italiana di Paleontologia e Stratigrafia 118, pp. 85-130.*

Noyan, Ö.F. & Vrielynck, B. (2000): Importance of morphogenetic analysis in taxonomy: an example from Triassic platform conodonts. *Neues Jahrbuch für Geologie und Paläontologie Monatshefte 2000(10), pp. 577-594.*

Orchard, M.J. (1991): Upper Triassic conodont biochronology and new index species from the Canadian Cordillera. *pp. 299-335. In: Orchard, M.J. & McCracken, A.D. (eds.): Ordovician to Triassic conodont paleontology of the Canadian Cordillera, Bulletin of the Geological Survey of Canada 417, p. 335.*

Paradis, E. & Schliep, K. (2019): Ape 5.0: an environment for modern phylogenetics and evolutionary analyses in R. *Bioinformatics 35(3), pp. 526-528.*

Pazonyi, P. & Virág, A. (2019a): Landmark analysis of *S. citelloides* (Sciuridae, Rodentia). *pp. 60. In: Hatvani, I.G., Tanos, P. & Fedor, F. (eds.): International Congress on Geomathematics in Earth and Environmental Sciences, Pécs Regional Committee of the Hungarian Academy of Sciences, p. 65.*

Pazonyi, P. & Virág, A. (2019b): A *Spermophilus citelloides* (Sciuridae, Rodentia) filogenetikai vizsgálata landmark analízis segítségével. *pp. 30. In: Bosnakoff, M. & Főzy, I. (eds.) Programok, előadások, kirándulásvezető. 22. Magyar Őslénytani Vándorgyűlés, Döbrönte, Magyarhoni Földtani Társulat, Budapest, p. 72.*

Pazonyi, P., Virág, A., Podani, J. & Pálfy, J. (2018): *Microtus* (*Microtus*) *nivaloides* from the Somssich Hill 2 site (southern Hungary): An Early Pleistocene forerunner of modern 'true' *Microtus* voles revealed by morphometric analyses. *Quaternary International 481, pp. 61-74.*

Pazonyi, P., Szabó, B. & Virág, A. (2020): Landmark alapú módszer zománcdifferenciáció és ontogenetikus változások nyomozására sztyeppi lemmingek (Lagurini) őrlőfogának példáján. *pp. 24-25. In: Bosnakoff, M., Szives, O. & Főzy, I. (eds.) Programok, előadások, kirándulásvezető. 23. Magyar Őslénytani Vándorgyűlés, Budapest, Magyarhoni Földtani Társulat, Budapest, p. 30.*

Popova, L., Maul, L.C. & Pazonyi, P. (2021): Biotic evolution and palaeogeography during the Quaternary with special reference to ground squirrels. *Historical Biology 33(1), pp. 1-3.*

Potočnik, B. (2015): Automated landmark points detection by using a mixture of approaches: the vole-teeth case. *Signal, Image and Video Processing 9, pp. 93-104.*

R Core Team (2013): R: A language and environment for statistical computing. *R*

Foundation for Statistical Computing, Vienna, Austria. https://www.R-project.org/

Sinitsa M.V., Pogodina, N.V. & Ryuchkova, L.Y. (2019): The skull of *Spermophilus nogaici* (Rodentia: Sciuridae: Xerinae) and the affinities of the earliest Old World ground squirrels. *Zoological Journal of the Linnean Society 186, pp. 826-864.*

Sinitsa, M.V., Virág, A., Pazonyi P. & Knitlová, M. (2021): Redescription and phylogenetic relationships of Spermophilus citelloides (Rodentia: Sciuridae: Xerinae), a ground squirrel from the Middle Pleistocene – Holocene of Central Europe. *Historical Biology 33(1), pp. 19-39.*

Smith, S.W. (2002): Digital signal processing: A practical guide for engineers and scientists. *Elsevier, p. 650.*

Schlager, S. (2017): Morpho and Rvcg – shape analysis in R: R-packages for geometric morphometrics, shape analysis and surface manipulations. *pp. 217-256. In: Zheng, G., Li, S. & Székely, G. (eds): Statistical shape and deformation analysis. Academic Press, p. 488.*

Szabó, B. & Virág, A. (2019a): Deer hunt in the random forest. *pp. 61. In: Hatvani, I.G., Tanos, P. & Fedor, F. (eds.): International Congress on Geomathematics in Earth and Environmental Sciences, Pécs Regional Committee of the Hungarian Academy of Sciences, p. 65.*

Szabó, B. & Virág, A. (2019b): A ságvári rénszarvasvadászok környezetének és vadászati stratégiájának rekonstrukciója. *pp. 35-36. In: Bosnakoff, M. & Főzy, I. (eds.) Programok, előadások, kirándulásvezető. 22. Magyar Őslénytani Vándorgyűlés, Döbrönte, Magyarhoni Földtani Társulat, Budapest, p. 72.*

Virág, A. & Karádi, V. (2022): Landmark point based and elliptic Fourier analysis of selected Lower Norian (Upper Triassic) conodonts: fundamentals, hinderances and perspectives of the different methods. *pp. 19. In: Jarochowska, E., Guenser, E. & Shirley, B. (eds): Abstract Book of the European Conodont Symposium, Utrecht, p. 27.*

Virág, A. & Karádi, V. (2023): Potential of closed contour analysis for species differentiation and holotype designation: a case study on lower Norian (Upper Triassic) conodonts. *Palaeontology 66(2), e12649.*

Virág, A. & Pazonyi, P. (2018): How landmark analysis can help unraveling the phylogenetic relationships of ground squirrels? *pp. 33. In: Váczi, O. & Németh, A. (eds.): Book of Abstracts of the VII. European Ground Squirrel Meeting & Subterranean Rodents Workshop, Budapest, Hungary, p. 79.*

Virág, A., Szabó, B. (2019): Computer-assisted edge detection and point acquisition: The future of landmark analysis? *pp. 126 In: Program and abstracts of the XVII Conference of the European Association of Vertebrate Palaeontologists, Brussels, p. 138.*

Virág, A., Szabó, B., Karádi, V. & Pazonyi, P. (2019a): Automated landmark analysis: a new methodology. *pp. 18. In: Hatvani, I.G., Tanos, P. & Fedor, F. (eds.): International Congress on Geomathematics in Earth and Environmental Sciences, Pécs Regional Committee of the Hungarian Academy of Sciences, p. 65.*

Virág, A., Szabó, B., Karádi, V. (2019b): Landmark based geometric morphometric analysis of selected Lower Norian conodonts. *pp. 65. In: Petti, F.M., Innamorati, G., Carmina, B. & Germani D. (eds.): Abstract Book of the 3rd International Congress on Stratigraphy, Milano, Società Geologica Italiana, Roma, p. 472.*